CHARACTERIZATION OF POROUS STRUCTURE AND ITS CORRELATION TO SODIUM EXPANSION OF GRAPHITE CATHODE MATERIALS USING IMAGE ANALYSIS

Xiang Li, Jilai Xue and Tong Chen
School of Metallurgical and Ecological Engineering, University of Science and Technology Beijing
Xueyuan Road 30, 100083 Beijing, China

Keywords: Porous structure, Image analysis, Cathode, Sodium expansion.

Abstract

Graphite cathode materials used in aluminum reduction cells are of porous structure. During aluminum electrolysis, the melt and sodium will penetrate into the cathode block leading to its expansion and deterioration. This work is aimed to give a better understanding of the relationship between the pore structure and the sodium expansion and to improve control of the cathode quality through quantitative image analysis.

Experiments with graphite cathode materials were carried out using a modified Rapoport apparatus. Image analysis results indicate that the porosity, pore diameter and pore connectivity after electrolysis can be related to the sodium expansion, while the aspect ratio and the fractal dimension seem to be unchanged. X-ray Diffraction (XRD) measurement for interlayer spacing (d 002) was also found to correlate to the degree of such expansion. Quantitative information on the correlation between the sodium expansion and porous structures can serve both the cathode producer and the smelter for product selection and performance evaluation of cathode blocks.

Introduction

During aluminum electrolysis, metallic sodium is generated and penetrated into carbon cathodes. The main mechanism for sodium penetration is diffusion of sodium into the carbon microstructures, which can result in sodium-carbon intercalation and expansion of cathode materials [1-2]. This is a major cause for generating internal stresses and cracks, shortening the service life of carbon cathodes.

In order to evaluate and control the cathode quality, the Rapoport test is applied to measure the sodium expansion of the cathode materials during aluminum electrolysis [3-4]. The degree in sodium expansion may vary with many influencing factors such as graphite content, time, electrolyte composition, current density, etc [5-6]. Based on the Rapoport test data, a constitutive model to reproduce the relationship between the sodium expansion and electrolysis time has been established for cathode carbon materials [7]. The diffusion coefficient, the distribution of sodium concentration, the varying stress in the cathode body can be described using this model.

Figure 1 is the comparison between experimental and numerical results of the sodium expansion from Zolochevsk's work. The cathode here was not considered as porous solid but as a continuous, uniform medium. It can be found that the expansion speed on the experimental curves is faster than those on numerical simulations, which could be due to a slower sodium expansion caused by the pore transformation during the electrolysis process. Figure 2 also shows that the sodium expansion rate is lower in experimental curves than in the modeling simulation [8]. These facts suggest that the pores in cathode carbons may play an important role in the expansion process. However, it is scarce in open scientific literature to deal with the correlation between cathode porosity and sodium expansion. Part of reason for this ignorance in scientific understanding may come from the lack of quantified and detailed investigative methods in the characterization of carbon porous structures.
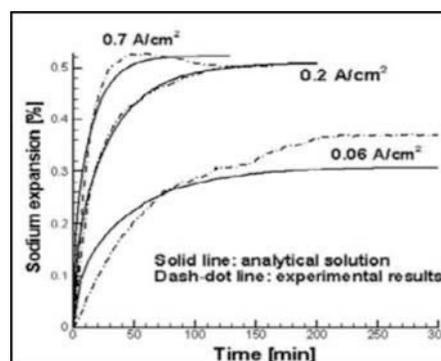
Figure 1. Variation of the sodium expansion with time in a solid cylinder with three values of a current density [7]
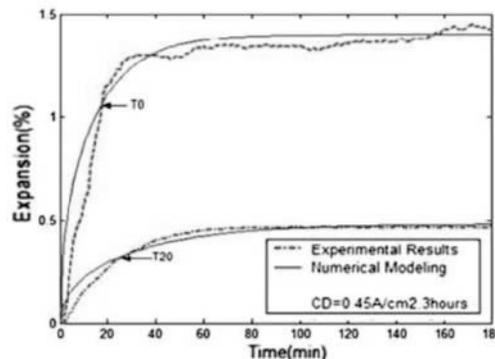
Figure 2. Comparison between experimental and numerical results of the sodium expansion [8]

Image analysis is a digital processing method for identifying, analyzing and explaining the contents of a photograph. Cooperating stereoscopy and quantitative metallography, the microstructure of materials can be characterized quantitatively [9-11]. This method has been used to quantify pores in cathode materials and interpret the melt penetration during aluminum electrolysis in correlation with pore properties [12-13].

This work is aimed to give a better understanding of the relationship between pore structure and sodium expansion. Pore structures of the cathode were investigated through quantitative

image analysis, while sodium expansion experiments with graphite cathode materials were carried out using a modified Rapoport apparatus.

Experimental

Figure 3 shows the experimental set-up for measuring sodium expansion during aluminum electrolysis, which is modified based on the Rapoport-Samoilenko apparatus [14]. The cylindrical cathode sample ($\Phi 25 \times 45$ mm) was fixed to the cathode rod by a mechanical thread. The expansion of the cathode sample during electrolysis was measured by a Laser Vertical Displacement (LVD) transducer (range 10 mm, resolution 1 µm) located on the top of the furnace. The signals obtained from the cathode expansion were logged once a minute to a PC connected to the LVD transducer. There was a corundum plate between the anode (graphite crucible) and the bottom of cathode sample, which functioned as an electrical isolation between them. The electrical current was passed from the anode rod, through the sidewall of the graphite crucible and molten electrolyte to the cathode sample.

The aluminum electrolysis was carried out at a temperature of 965 °C under an argon atmosphere. A constant current was generated by a MPS302 DC power supply and the cathode current density was 0.5 A/cm^2. The cryolitic ratio (molecular ratio of NaF/AlF$_3$) of the electrolyte was 4.0 containing 5 wt. % CaF$_2$ and 8 wt. % Al$_2$O$_3$. The tested cathodes were all 100 % graphite materials.

1-LVD transducer; 2-Cathode rod; 3-Gas outlet;
4- Graphite crucible (as anode);
5- Cryolite melt; 6-Cathode sample; 7-Alsint support;
8-Furnace; 9-Anode rod; 10- Gas inlet
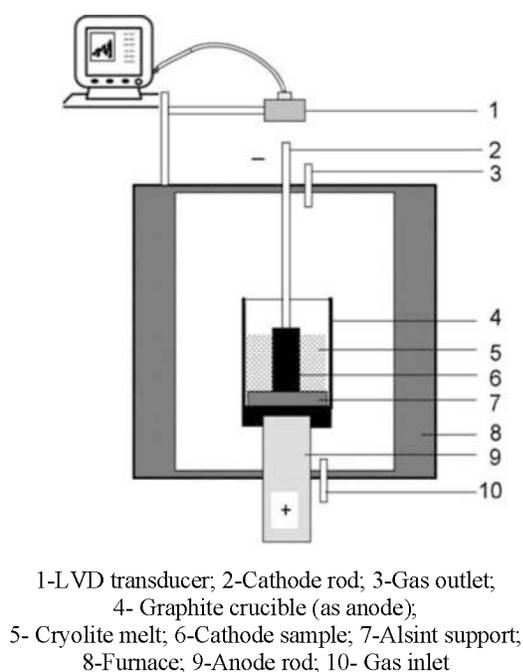
Figure 3. Experimental set-up for measuring sodium expansion in aluminum electrolysis

After electrolysis, the cathode samples were lifted to the upper position of furnace. The samples after cooling to ambient temperature were cut off and ground for photographing. Regions from each sample under inspection were captured for image analysis of the pores parameters by the method as described in the previous paper [13]. All pores parameters calculated were performed by using Image J software. Furthermore, XRD analysis

was also applied to identify the interlayer spacing (d 002) of cathode carbon.

Results and Discussion

The Pore Structures of Cathode in Different Expansion Stage

In Figure 4, a comparison of binary images obtained by polarization microscope for four cathode materials is shown. Of these, GSM-0 represents a cathode sample with no electrolysis, where it can be seen that the pores are small, with homogeneous dispersion and not presenting specific orientation; GSM-1 is the cathode after electrolysis for 15 min, GSM-2 for 30 min and GSM-3 for 150 min. The four specimens were taken from the cathode samples corresponding to 1) no electrolysis, 2) half-way period, 3) arrived just in balance period, and 4) balance period, on expansion curve as shown in Figure 5.
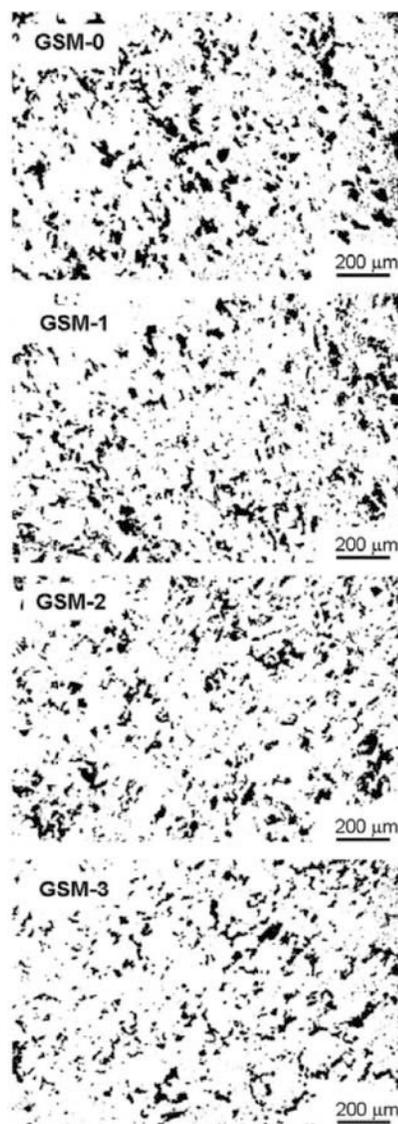
Figure 4. Binary image of graphite cathode materials before and after aluminum electrolysis

Table I. Statistical Results of Image Analysis on the Pores in Cathode Samples

Sample No.	Electrolysis Time(min)	Porosity (%)	Aspect	Mean Diameter (μm)	Fractal Dimension	Connectivity (%)
GSM-0	0	13.89	2.03	16.46	1.117	12.09
GSM-1	15	13.31	2.00	15.10	1.115	9.01
GSM-2	30	11.85	2.01	15.01	1.114	7.96
GSM-3	150	11.60	2.05	15.10	1.122	7.44
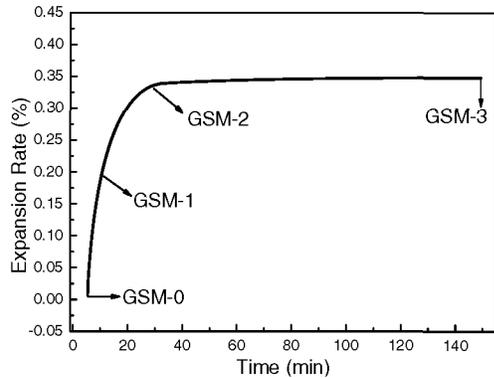
Figure 5. A typical curve illustrating the various stages during sodium expansion process vs. electrolysis time

The porous structure parameters used in this paper were explained as follows: Porosity is the ratio of pore area to the total region area; Aspect is the ratio of the major diameter and the minor diameter of an ellipse equivalent to a pore; Mean Diameter is the average length of diameters measured at 2 degree intervals and passing through the pore centroid; Fractal Dimension is the fractal dimension of the pore outline; Connectivity is calculated from the percentage of connecting lines' length to total objects' length in skeletonization.

Table I shows the results of the image analysis corresponding to the samples in Figure 4. The porosity of the no electrolysis sample GSM-0 was 13.89 %. The porosity of sample GSM-1 which under went 15 min electrolysis decreased slightly, but diameter and connectivity decreased obviously. Sample GSM-2 with 30 min electrolysis showed an obvious decrease in porosity, diameter and connectivity. After 150 min electrolysis, the parameters of cathode pores also decreased substantially. However, aspect and fractal dimension became smaller firstly, and then increased. The porous structure variation may be due to metallic sodium and electrolyte melt penetrated into cathode sample, which would be further discussed afterwards.

Figure 6 shows the changing of the pore structure parameters with electrolysis time. The porosity decreased with increasing electrolysis time. At the half-way stage of the sodium expansion period, the porosity decreased 0.58 %. When the expansion achieved balance, porosity exhibited a lower total porosity and decreased 1.94 %. After 120 min, porosity had reduced by 2.29 % when compared to no electrolysis. With increasing electrolysis time, connectivity also decreased. It decreased 4.55 % after electrolysis of 150 min. The diameter decreases at half-way stage and just arrived at balance stage, while it became a little higher

after expansion balance 120 min. The change of pore size may be due to the disappearance of tiny pores after expansion resulting in the number of pores decreasing and the mean diameter increasing. This can be proved from the results of the pore size distributions.
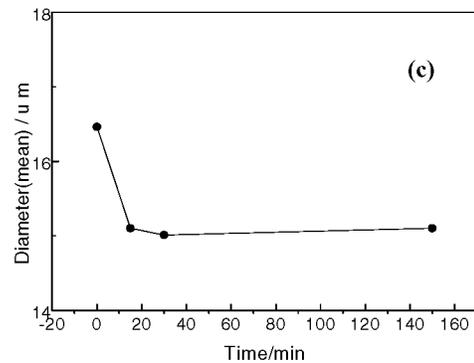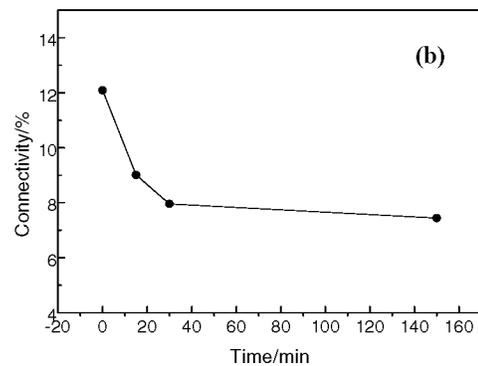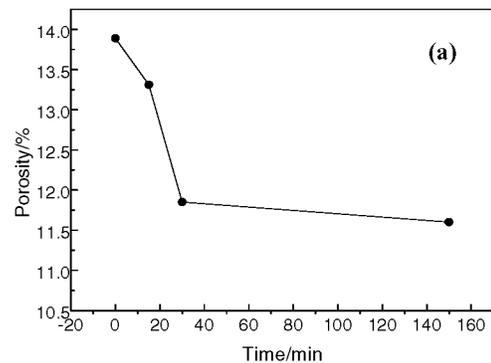
Figure 6. Variation of pore structures with electrolysis time. (a) is the porosity variation with the electrolysis time; (b) is the connectivity variation with the electrolysis time; (c) is the mean diameter of pores variation with the electrolysis time.
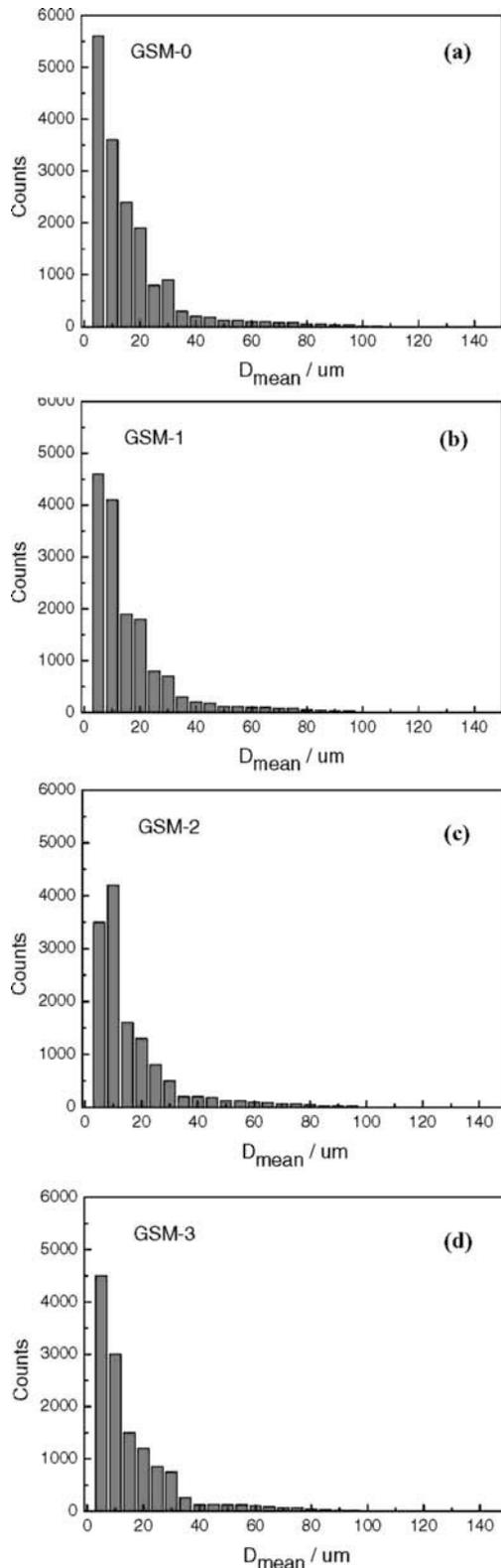
Figure 7. Pore size distributions for cathode samples before and after electrolysis. (a) is the no electrolysis sample's pore size distribution; (b), (c), (d) are the samples' for electrolysis 15 min, 30 min, 150 min respectively.

In Figure 7, pore size distributions for cathode samples before and after electrolysis are shown. Pores of diameter under 5 μm are the majority before electrolysis, but their number decreases with increasing time. The number of pores in the 10 μm-60 μm diameter range decreases a little after electrolysis, while pores above 60 μm have no change within 30 min electrolysis time. After 150 min electrolysis, the number of big pores decreases a little and their size would become smaller than before, while some small pores may disappear. So the volume sum of all size pores may be compressed during sodium expansion.

In general, all results of image analysis show that the change of porous structures can mainly occur during the stage of increased expansion. After expansion is balanced, the change in pore structure becomes small and the structures become stable. The difference between the numerical simulation and experimental data found in Zolochevsk's work is also the same period as the increased expansion. The obtained results indicate that the pores can make impact on the cathode expansion, which should not be ignored when understanding the sodium expansion mechanism.

XRD Characterization

Table II shows the C/C interlayer spacing values calculated from the XRD results for comparisons of microstructural change related to the expansion ratio. It can be seen the value of C/C interlayer becomes larger after electrolysis. However, the differences of C/C interlayer among GSM-1, GSM-2 and GSM-3 were very small, indicating the majority of the increase in C/C interlayer spacing occurred during the period of electrolysis prophase.

Table II. Carbon Interlayer Spacing Values – d(002)

Sample	Electrolysis Time(min)	d(002) (Å)
GSM-0	0	3.3627
GSM-1	15	3.3754
GSM-2	30	3.3757
GSM-3	150	3.3728

Pore Deformation Mechanism and its Effect on Sodium Expansion

In the Heroult-Hall reduction process, Al^{3-} diffuses into the boundary layer of the cathode, and corresponding Na^+ must be accompanied in order to keep electric neutrality. When the Al^{3-} turns to metallic aluminum, generated F^- is combined with Na^+ and turns into NaF. NaF therefore enriches near the cathode surface, which cause an increase in local CR of the melt. Two reactions may happen:

$$Na^+ + e^- = Na \qquad (1)$$

$$Al + 3NaF = 3Na + AlF_3 \qquad (2)$$

Thonstad and Rolseth [15] measured the overvoltage at 1010 °C at different CR and CD (current density). Eq. (3) could be fitted to the data obtained

$$\eta = \frac{RT}{F}\ln\left(\frac{a_{Na}}{a_{Na}^*}\right)^{1283k} \approx 0.25 + 0.028 \cdot CR - (0.31 - 0.031 \cdot CR)\log(CD) \qquad (3)$$

Where a_{Na} and a^*_{Na} are the activities of sodium in the bulk melt and at the aluminum surface, respectively. The overvoltage was calculated equal to 0.403 V for testing conditions, suggesting possible generation of metal Na in the experiments.

XRD results show the d(002) spacing values increase by 0.3 – 0.4 % due to sodium expansion, and the partial expansion in the cathode can result in internal stress developing deformation of the pores. Under this pressure, the round pores would turn long and narrow, so that the pore volume reduces while the connectivity remains the same. The original long and narrow pores could come into contact at the narrow points to become two or more pores under the pressure, thus deceasing their connectivity and pore diameter. At the stage of expansion balanced (see Figure 5), the inner stress in carbon cathode continues to release and results in small change in pore structures. With increasing electrolysis time, the electrolyte melts start penetrating into the cathode to occupy the pores space. The samples after electrolysis were polished for photographs and the electrolyte in big pores may have been easy to remove during polishing while may retain in the small pores, so the number of small pores would still decrease at the stage of expansion balanced.
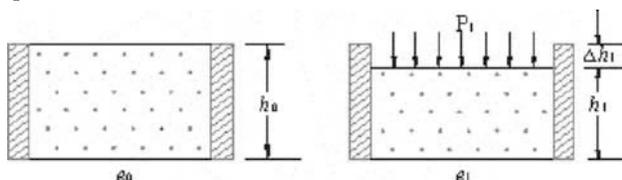
Figure 8. Schematic drawing of pores space compressed

Figure 8 illustrates that all internal stresses of carbon are supposed to be an external pressure marked as P_1. Assume the cross sectional area of samples before electrolysis as A, and the height as h_0. The space of pores is compressed under the press P_1, so the height decreases by $\triangle h_1$ to h_1, while the porosity reduces from e_0 to e_1. Under the hypothesis of sample diameter being unchanged, the volume of carbon materials would be the same before and after electrolysis, which could be shown as Equation (4).

$$\frac{Ah_0}{1+e_0} = \frac{A(h_0 - \triangle h_1)}{1+e_1} \qquad (4)$$

Thus, Equation (4) can be transformed to:

$$\frac{\triangle h_1}{h_0} = \frac{e_0 - e_1}{1+e_0} \qquad (5)$$

Because the pores in cathode sample can release part of internal stress, the total expansion rate would decrease. Equation (5) is just the different part in expansion rate between the cathode containing pores and the ideal solid cathode.

Conclusions

1. The difference of porous structures before and after sodium expansion can be distinguished by image analysis methods, demonstrating an effective approach to characterize the pore deformation due to sodium expansion.

2. Image analysis results indicate that there is a porosity, mean diameter, and connectivity decrease with increasing electrolysis time, while the aspect ratio and the fractal dimension seem to be unchanged.

3. The change of porous structures mainly occurs during the stage of increased expansion and after expansion is balanced the change in pores becomes small with stable structures.

4. Due to the space of pores compressed under the internal stress, the total expansion rate of the cathode sample is lower than that of the ideal solid cathode.

References

1. M. Sorlie and H. A. Øye, *Cathodes in Aluminium Electrolysis* (Aluminium-Verlag), 1994, 127-132.

2. L. P. Lossius and H. A. Øye, "Melt Penetration and Chemical Reactions in 16 Industrial Aluminum Carbon Cathodes," *Metallurgical and Materials Transactions B*, 31B (12) (2000), 1213-1224.

3. D. S. Newman et al, "A Technique for Measuring In Situ Cathode Expansion (Rapoport Test) during Aluminum Electrolysis," *Light Metals 1986*, 1986, 685-688.

4. A. Zolochevsky et al, "Creep and Sodium Expansion in a Semigraphitic Cathode Carbon," *Light Metals 2003*, 2003, 602.

5. J. G. Hop, "Sodium Expansion and Creep of Cathode Carbon," (Ph.D. thesis, Norwegian University of Science and Technology, 2003), 90-103.

6. J. M. Peyneau and J. R. Gaspard, "Laboratory Testing of the Expansion under Pressure due to Sodium Intercalation in Carbon Cathode Materials for Aluminium Smelters," *Light Metals 1992*, 1992, 801-808.

7. A. Zolochevsky et al, "Rapoport–Samoilenko Test for Cathode Carbon Materials I. Experimental Results and Constitutive Modeling," *Carbon*, 41 (2003), 497–505.

8. J. Xue, Q. Liu and W. Ou, "Sodium Expansion in Carbon /TiB$_2$ Cathodes during Aluminum Electrolysis," *Light Metals 2007*, 2007, 1061-1066.

9. S. Rorvik, H. A. Øye and M. Sorlie, "Characterization of Porosity in Cokes by Image Analysis," *Light Metals 2001*, 2001, 601-609.

10. S. Rorvik, A. P. Ratvik and T. Foosnas, "Characterization of Green Anode Materials by Image Analysis," *Light Metals 2006*, 2006, 553-558.

11. J. G. Hop and H. A. Øye, "In-Situ Strength Reduction of Anthracitic Cathode Carbon and Crack Quantifying by the Use of Image Analysis," *Light Metals 2001*, 2011, 717-722.

12. Y. Gao et al, "Characterization of Sodium and Fluoride Penetration into Carbon Cathodes by Image Analysis and SEM-EDS Techniques," *Light Metals 2011*, 2011, 1103-1107.

13. X. Li et al, "Analysis of Porous Structures of Graphitic Cathode Materials and the Correlation to Penetrated Sodium," *Light Metals 2012*, 2012, 1319-1324.

14. M. B. Rapoport and V. N. Samoilenko, "Deformation of Cathode Blocks in Aluminium Baths during Process of Electrolysis," *Tsvet Met*, 30 (2) (1957), 44-51.

15. J. Thonstad and S. Rolseth, "On the Cathodic Overvoltage on Aluminium in NaF - AlF$_3$ - Al$_2$O$_3$ Melts – II," *Electrochimica Acta*, 23 (1978), 233-241.